International Journal of
Metallurgical & Materials Engineering
Research Article Open Access
Special Issue: Bioceramics: Designing, Applications and Challenges

Control of Ca/P Molar Ratio of Plate-shaped Hydroxyapatite Powders With an *a*(*b*)-axis Orientation and Their Thermal Stability

Yuki Mori and Mamoru Aizawa*
Department of Applied Chemistry, School of Science and Technology, Meiji University, 1-1-1 Higashimita, Tama-ku, Kawasaki 214-8571, Japan

Abstract

Hydroxyapatite is one of main inorganic constituents of human bones and teeth. It is widely used as a biomaterial due to its great bioactivity and biocompatibility. The hydroxyapatite crystals have two kinds of crystal axes: an *a*(*b*)-axis and a *c*-axis. There are some advantages in the hydroxyapatite crystals with an *a*(*b*)-axis orientation. In recent years, a synthesis method has been reported for plate-shaped hydroxyapatite powders with an *a*(*b*)-axis orientation. However, the Ca/P molar ratio of the synthesized powders was lower than that of hydroxyapatite with stoichiometric composition. For this reason, they were thermally decomposed into β-tricalcium phosphate over 700°C. In order to solve the problem, we utilized dissolution-deposition reactions caused by hydrothermal treatment. In this study, the hydrothermal treatment was performed with variation of two hydrothermal conditions: Ca^{2+} ion concentration and hydrothermal temperature. Furthermore, we examined a thermal stability by heating the hydrothermal-treated powders at 1000°C for 1 h. When the synthesized powders were hydrothermally treated at 180°C for 2.5 h in a calcium chloride solution (1.0 mol•dm^{-3}), the Ca/P molar ratio of them increased from 1.38 to 1.64. In addition, the optimized hydroxyapatite powders were the thermally stablest among examined samples still after heating. From the above, the hydrothermal process is considered to be useful for the preparation of the plate-shaped hydroxyapatite powders with closer stoichiometric Ca/P molar ratio and the development of their thermal stability.

Publication History:
Received: January 17, 2017
Accepted: March 14, 2017
Published: March 16, 2017

Keywords:

Hydroxyapatite, Ca-deficient hydroxyapatite, Anisotropy control, Morphology control, Air-liquid interface process, Hydrothermal treatment, Powder X-ray diffraction

Introduction

Hydroxyapatite ($Ca_{10}(PO_4)_6(OH)_2$; HAp) is one of constituent compounds of human bones and teeth [1,2]. HAp has a good bioactivity and biocompatibility. Therefore, it is widely used as a biomaterial [3]. Its crystal structure belongs to hexagonal system and has two kinds of crystal planes: a-planes with positive charge and c-planes with negative charge [4-6]. Thus, it is also utilized as an adsorbent for chromatography [7].

The crystal axes of HAp crystals consist of an *a*(*b*)-axis and a c-axis [8]. Crystal growth along the *a*(*b*)-axis results in HAp crystals with a plate-shaped morphology (Figure 1). The HAp crystals with the *a*(*b*)-axis orientation have large c-planes, described as a miller index of (00l). Hence, they acquire specific adsorption property for basic proteins. Similarly, the HAp crystals with the c-axis orientation acquire specific adsorption property for acidic proteins. In addition, the HAp crystals in long bones of humans and animals have the c-axis orientation, whereas those in tooth enamel of humans and animals have the *a*(*b*)-axis orientation [9,10]. It still has not been revealed that why the biological HAp has such a difference. With the aim of solving the question, textured HAp ceramics are required as a model for human long bones and tooth enamel. Therefore, it is important to impart different orientations to the HAp crystals.

Until now, many studies have been reported about a synthesis method for fiber-shaped HAp powders with the c-axis orientation. Aizawa et al. [11, 12] prepared the HAp fibers with well-controlled Ca/P molar ratio using a homogeneous precipitation process. Yoshimura et al. [13] and Zhu et al. [14] reported that the HAp fibers can be produced with a hydrothermal process. Zhang et al. [15,16] synthesized the HAp fibers by combining a homogeneous precipitation process and a hydrothermal process. On the other hand, there are only a few reports about a synthesis method for plate-shaped HAp powders with the *a*(*b*)-axis orientation. Ban et al. [17,18] prepared the plate-shaped HAp powders on titanium substrates using an electrochemical process (not powder synthesis). Yamamoto et al. [19] reported that the plate-shaped HAp powders can be produced by a homogeneous precipitation process involving hydrolysis reactions of urea with urease. However, the resulting powders were discovered to be polycrystals.

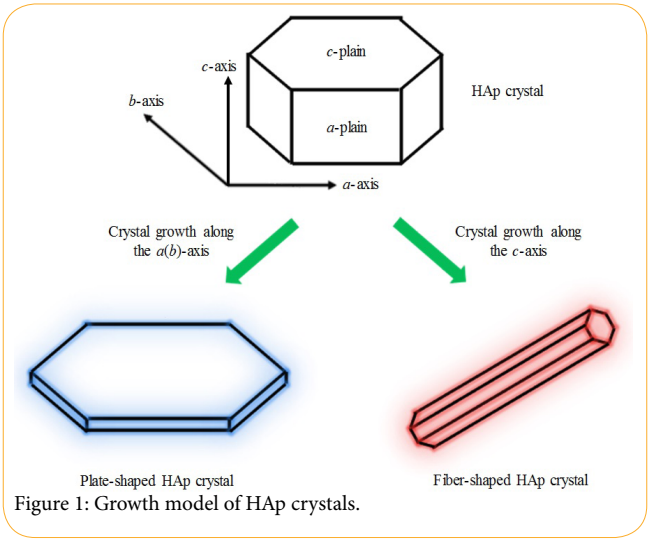

Figure 1: Growth model of HAp crystals.

***Corresponding Author:** Dr. Mamoru Aizawa, Department of Applied Chemistry, School of Science and Technology, Meiji University, 1-1-1 Higashimita, Tama-ku, Kawasaki 214-8571, Japan, Tel: +81-44-934-7237; E-mail: mamorua@meiji.ac.jp

Citation: Mori Y, Aizawa M (2017) Control of Ca/P Molar Ratio of Plate-shaped Hydroxyapatite Powders With an *a*(*b*)-axis Orientation and Their Thermal Stability. Int J Metall Mater Eng 3: 132. doi: https://doi.org/10.15344/2455-2372/2017/132

Some researchers reported that "single crystal" platelets with hexagonal shapes could be synthesized at the air-liquid, liquid-liquid and solid-liquid interfaces [20-23]. Based on the reports, Zhuang et al. [24] succeeded in synthesizing HAp powders by utilizing air-liquid interfaces of a reaction solution. In a scanning electron microscope (SEM) image, the resulting powders had a hexagonal plate-shaped morphology. In addition, observations using a transmission electron microscope illustrated that the resulting powders were single crystal. However, the resulting powders were found to be Ca-deficient Hap and thermally decomposed into β-tricalcium phosphate (β-$Ca_3(PO_4)_2$; β-TCP) over 700°C due to their nonstoichiometric composition.

In order to solve the above problem, we performed the control of the Ca/P molar ratio of the Ca-deficient HAp powders with hexagonal shapes via hydrothermal reactions route. The hydrothermal reactions have been utilized for preparing various nanomaterials and surface modifications [25]. Furthermore, the HAp crystals are repeatedly dissolved and deposited, when hydrothermally reacting in a solution. Utilizing the dissolution-deposition reactions makes it possible to increase Ca/P molar ratio of the single crystal plate-shaped HAp powders, because Ca-deficient HAp crystals dissolve and stoichiometric HAp crystals deposit. In this study, the single crystal plate-shaped HAp powders were hydrothermally treated with variation of two parameters: Ca^{2+} ion concentration and hydrothermal temperature to characterize their powder properties. Moreover, we examined a thermal stability of the hydrothermal-treated powders.

Materials and Methods

Preparation of the plate-shaped HAp powders with an *a*(*b*)-axis orientation

The single crystal plate-shaped HAp powders were synthesized by air-liquid interface process [24]. Briefly speaking, a 500 cm^3 solution of 3.0 mmol•dm^{-3} phosphoric acid (H_3PO_4; Wako Pure Chemical Industries, Ltd., Japan) was dripped into a 500 cm^3 solution of 5.0 mmol•dm^{-3} calcium carbonate ($CaCO_3$; Wako Pure Chemical Industries, Ltd., Japan) and 1.0 mol•dm^{-3} urea ($(NH_2)_2CO$; Wako Pure Chemical Industries, Ltd., Japan). The dripping rate was 6 cm3•min^{-1}. After stirring the mixed solution for 2 h, a nitric acid solution (HNO_3; Wako Pure Chemical Industries, Ltd., Japan) was added to adjust a pH value of the solution to 3.0. Next, the solution was agitated for 2 h again. Finally, a 2.734 cm^3 solution of 0.1 mass% urease (from Jack Bean, Wako Pure Chemical Industries, Ltd., Japan) was added, and the solution was stirred for 15 min. After dispensing the starting solution (120 cm^3) in a glass petri dish (116 mm), it was heated in an incubator (SIW-300, AS ONE, Co., Japan) at 50°C for 96 h. Hydrolysis reactions of urea (substance) proceed on the co-presence of urease (enzyme) in the first step, and thenthe pH value of the reaction solution increases to become basic [19].Finally, white products were obtained at air-liquid interfaces of the reaction solution. They were collected and dried at 110°C for 24 h.

Control of the Ca/P molar ratio of the plate-shaped HAp powders by the hydrothermal treatment

In order to increase the Ca/P molar ratio of the single crystal plate-shaped HAp powders, the hydrothermal treatment was carried out. 0.03 g of the synthesized powder was put in a hydrothermal device (TVS-1, TAIATSU TECHNO, Co., Japan) along with a 10 cm^3 calcium chloride ($CaCl_2$; Wako Pure Chemical Industries, Ltd., Japan) solution. Ultrapure water was used as a "solution of 0 mol•dm^{-3} $CaCl_2$".An inner cylinder made of polytetrafluoroethylene was used as a container. Finally, the hydrothermal device was heated in an oil bath (HBR 4 digital, IKA-Werke, GmbH and Co.KG, Germany). After cooling the hydrothermal device to room temperature by the water, the hydrothermal-treated powders were collected and dried at 110°C for 24 h. For the purpose of determining optimal hydrothermal conditions, two kinds of parameters were varied, described in Table 1.

Section number	Ca^{2+} ion concentration / mol•dm^{-3}	pH value at the starting point	Hydrothermal temperature / °C	Hydrothermal time / h
3-2	0	6.53	120	2.5
	0.1	7.16	120	2.5
	0.5	8.12	120	2.5
	1.0	8.98	120	2.5
3-3	1.0	9.12	100	2.5
	1.0	9.15	120	2.5
	1.0	9.03	140	2.5
	1.0	9.09	160	2.5
	1.0	9.09	180	2.5

Table 1: Preparation conditions for plate-shaped HAp powders with well-controlled Ca/P molar ratio.

Characterization of the plate-shaped HAp powders

Crystal phases of the powders were identified by an X-ray diffraction (XRD) device (MiniFlex, Rigaku, Co., Japan) using a Cu-Kα radiation at 30 kV and 15 mA. The XRD data were collected under following conditions: 2θ range of 3-60°, scanning rate of 2°•min^{-1} and sampling width of 0.02°. The identification of the XRD peaks was carried out with a database of International Centre for Diffraction Data (ICDD; HAp: #00-009-432, OCP: #00-026-1056). Functional groups of the powders were investigated using a fourier transform infrared (FT-IR) spectroscope (IRPrestage-21, SHIMADZU Co., Japan). The FT-IR data were collected under conditions below: measurement mode of %Transmittance, apodization function of Happ-Genzel, wavenumber range of 400-4000 cm^{-1}, resolution of 4.0 cm^{-1} and cumulative number of 40 times. The investigation of the functional groups was performed by a potassium bromide pellet method. Particle morphologies of the powders were observed using a SEM (JSM-6390LA, JEOL, Ltd., Japan) with an accelerating voltage of 10 kV. Platinum coating was carried out on the powder surfaces before observing. Ca and P contents of the powders were determined by an inductively-coupled plasma atomic emission spectrometer (ICP-AES; SPS7800, Hitachi High-Tech Science, Co., Japan), and the Ca/P molar ratio of those was calculated. The determination of the atomic contents was performed under following conditions: radio-frequency output of 1.2 kW, measured Ca wavelength of 317.993 nm, measured P wavelength of 213.618 nm, integration time of 5 sec and integration number of 10 times.

Thermal stability of the hydrothermal-treated HAp powders

We examined effects of the Ca/P molar ratio of the plate-shaped HAp powders on their thermal stability. The synthesized powders and the hydrothermal-treated powders with variation of the hydrothermal temperature were heated in an electric furnace (KBF314N, Koyo Thermo Systems, Co., Ltd., Japan) at 1000 °C for 1 h in air. The heating rate was 10 °C•min-1. In addition to the evaluations using the XRD device, the FT-IR spectroscope, the SEM and the ICP-AES, ratio of

a HAp phase of the heated powders was calculated by a reference intensity ratio method on the basis of their powder XRD patterns using related peaks in the ICDD database (HAp: #01-072-1243, β-TCP: #01-072-7587).

Results and Discussion

Characterization of the synthesized powders

The powder XRD pattern, the FT-IR spectrum and the SEM image of the synthesized powders are shown in Figure 2. The synthesized powders were hexagonal HAp platelets with the *a*(*b*)-axis orientation. However, they were of HAp and octacalcium phosphate ($Ca_8(PO_4)_4(HPO_4)_2 \bullet 5H_2O$; OCP) bi-phases. For this reason, the Ca/P molar ratio of the synthesized powders was 1.39, although that of stoichiometric HAp is about 1.67.

Determination of the Ca^{2+} ion concentration for the plate-shaped HAp powders with well-controlled Ca/P molar ratio

This experiment was designed to clarify effects of the Ca^{2+} ion concentration on the preparation of the plate-shaped HAp powders with well-controlled Ca/P molar ratio. Figure 3 shows the powder XRD patterns of the hydrothermal-treated powders. Regardless of the Ca^{2+} ion concentration, they were of an HAp single phase due to conversion of the OCP phase. As shown in Figure 4, there was no difference between the spectrum of the synthesized powders and the spectra of the hydrothermal-treated powders. In the SEM images, the hydrothermal-treated powder particles exhibited a slightly broken morphology irrespective of the Ca^{2+} ion concentration (Figure 5). Table 2 listed the Ca/P molar ratio of the hydrothermal-treated powders. It was fairly close to 1.67 at the high Ca^{2+} ion concentration.
From the above, the Ca^{2+} ion concentration of 1.0 mol•dm^{-3} was the optimal condition in the range of examination of this study.

As shown in Figure 3, the peaks assigned to a HAp phase became stronger after the hydrothermal treatment (especially in the 2θ range of 31-33°) As stated above, the HAp crystals are repeatedly dissolved and deposited during the hydrothermal reactions. At the same time, the conversion of the OCP phase to the HAp phase also occurred. Hence, it is thought that the peaks were strengthened by the HAp crystals newly formed in the process of the hydrothermal reactions. Though the OCP crystals were converted to the HAp crystals by the hydrothermal reactions, a band at 950 cm^{-1} assigned to hydrogen phosphate (HPO_4^{2-}) ions was still detected (Figure 4). At first, HPO_4^{2-} ions generated from the OCP crystals may be dissociated into H+ ions and phosphate (PO_4^{3-}) ions, and then the generated PO_4^{3-} ions may be consumed to form the HAp crystals. However, the hydrothermal solution is expected to become acidicdue to the generated H+ ions. In fact, a pH value of the solution decreased to 3 or less at the end point. Then, it is assumed that the dissociation reaction of the HPO_4^{2-} ions gradually stopped proceeding. As these remained HPO_4^{2-} ions were

	Synthesized powders	Hydrothermal-treated powders			
		0 mol•dm^{-3}	0.1mol•dm^{-3}	0.5mol•dm^{-3}	1.0 mol•dm^{-3}
Ca/P molar ratio	1.39	1.55	1.56	1.56	1.57

Table 2: Ca/P molar ratio of the hydrothermal-treated powders at 120°C for 2.5 h in a $CaCl_2$ solution.

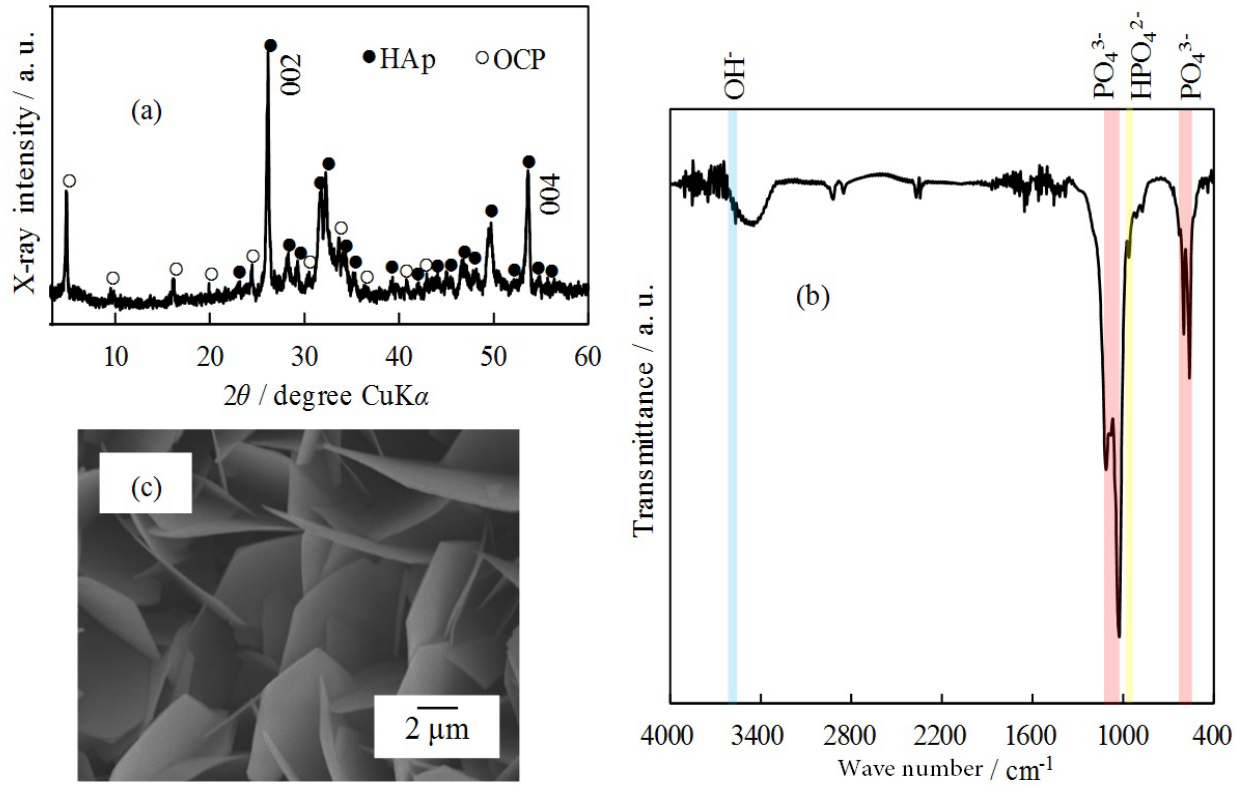

Figure 2: Characterization of the synthesized powders: (a) XRD pattern, (b) FT-IR spectrum and (c) SEM image.

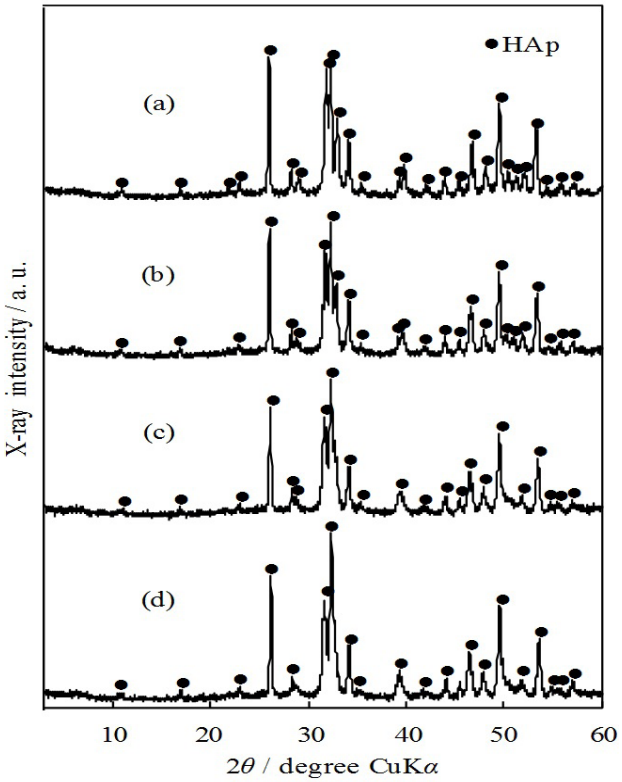

Figure 3: XRD patterns of the hydrothermal-treated powders at 120˚C for 2.5 h in a $CaCl_2$ solution: Ca^{2+} ion concentration (a) 0, (b) 0.1, (c) 0.5 and (d) 1.0 mol•dm^{-3}.

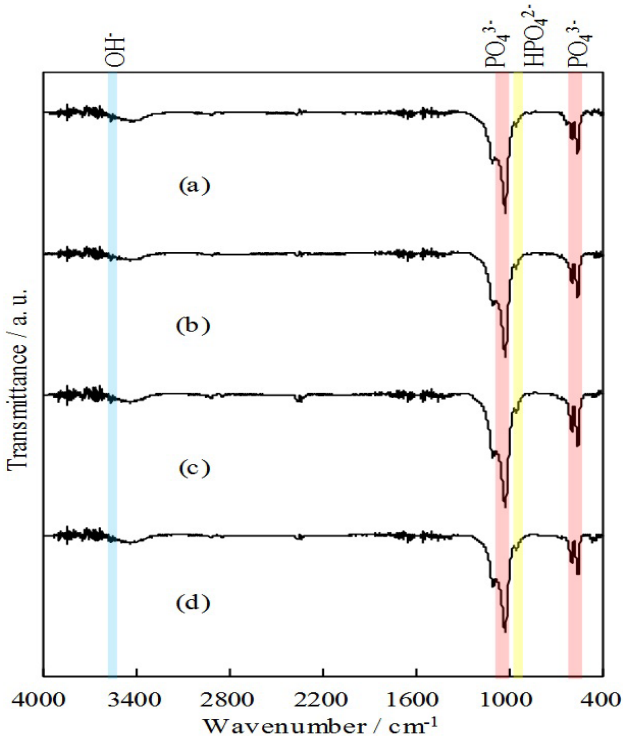

Figure 4: FT-IR spectra of the hydrothermal-treated powders at 120˚C for 2.5 h in a CaCl2 solution: Ca^{2+} ion concentration (a) 0, (b) 0.1, (c) 0.5 and (d) 1.0 mol•dm^{-3}.

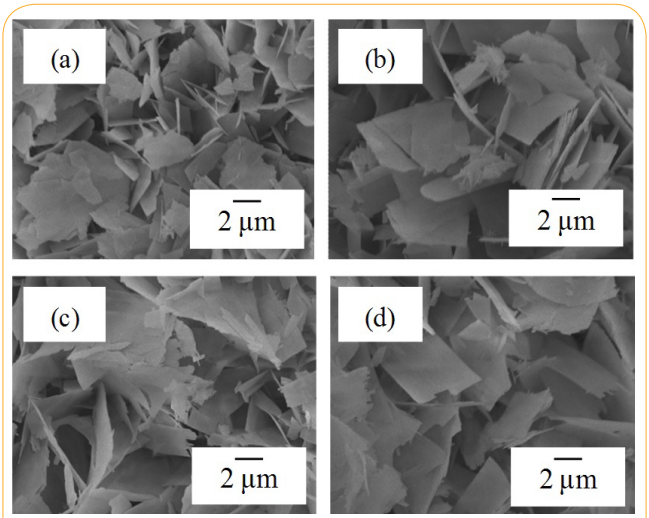

Figure 5: SEM images of the hydrothermal-treated powders at 120˚C for 2.5 h in a $CaCl_2$ solution: Ca^{2+} ion concentration (a) 0, (b) 0.1, (c) 0.5 and (d) 1.0 mol•dm^{-3}.

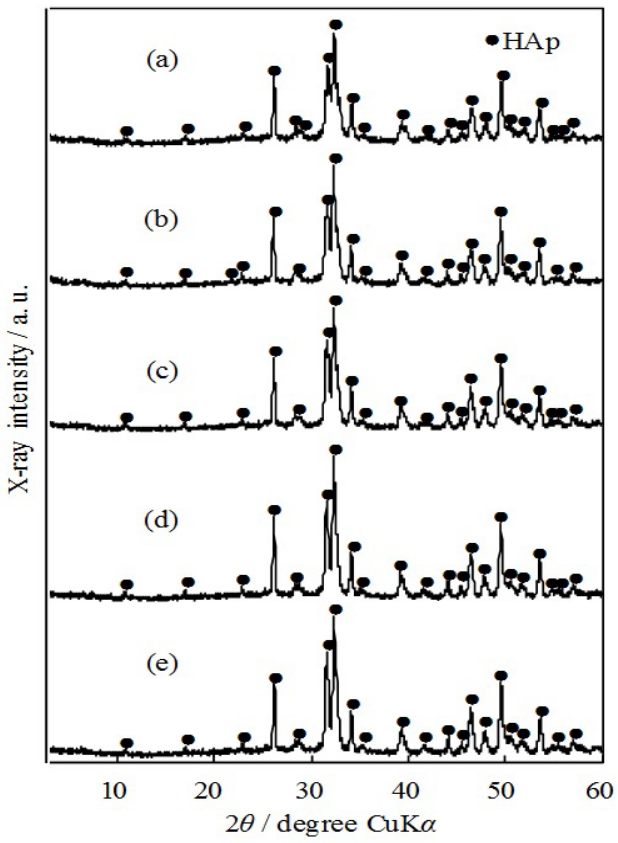

Figure 6: XRD patterns of the hydrothermal-treated powders for 2.5 h in a solution of 1.0 mol•dm^{-3} $CaCl_2$: hydrothermal temperature (a) 100, (b) 120, (c) 140, (d) 160 and (e) 180˚C.

directly incorporated in deposited HAp crystals, Ca-deficient HAp ($Ca_{10-x}(PO_4)_{6-x}(HPO_4)_x(OH)_{2-x}$) crystals may be formed in this work. As the hydrothermal reactions take place under high pressure conditions, the particle morphologies of the plate-shaped HAp crystals were slightly broken due to collision between the particles (Figure 5). As a result, the plate-shaped HAp crystals certainly became smaller. However, small fragments of the plate-shaped HAp crystals

also have a plate-shaped morphology. For this reason, we considered that the adverse effect of the hydrothermal treatment on the particle morphologies of the plate-shaped HAp crystals is not significant.

Effect of the hydrothermal temperature on the preparation of the plate-shaped HAp powders with well-controlled Ca/P molar ratio

This experiment was designed to reveal effects of the hydrothermal temperature on the preparation of the plate-shaped HAp powders with well-controlled Ca/P molar ratio. The powder XRD patterns, the FT-IR spectra and the SEM images of the hydrothermal-treated powders are shown in Figure 6, 7 and 8, respectively. These results were the same as those obtained in the section 3-2. As listed in Table 3, the Ca/P molar ratio of the hydrothermal-treated powders became closer to 1.67 with increasing the hydrothermal temperature. Thus, the hydrothermal temperature of 180°C was the best condition in the range of examination of this study.

With raising the hydrothermal temperature, the Ca/P molar ratio of the plate-shaped HAp powders became closer to 1.67 (Table 3). As mentioned above, the dissociation of the HPO_4^{2-} ions occurred in the process of the deposition of the HAp crystals. It is considered that the dissociation reaction proceeds further, as the hydrothermal temperature becomes higher. In other words, the higher the hydrothermal temperature is, the less the HPO_4^{2-} ions are in the solution with Ca^{2+} ions. As a result, the hydrothermal temperature of 180°C was the best for preparing the plate-shaped HAp powders with stoichiometric Ca/P molar ratio close to 1.67 in the examined experimental conditions.

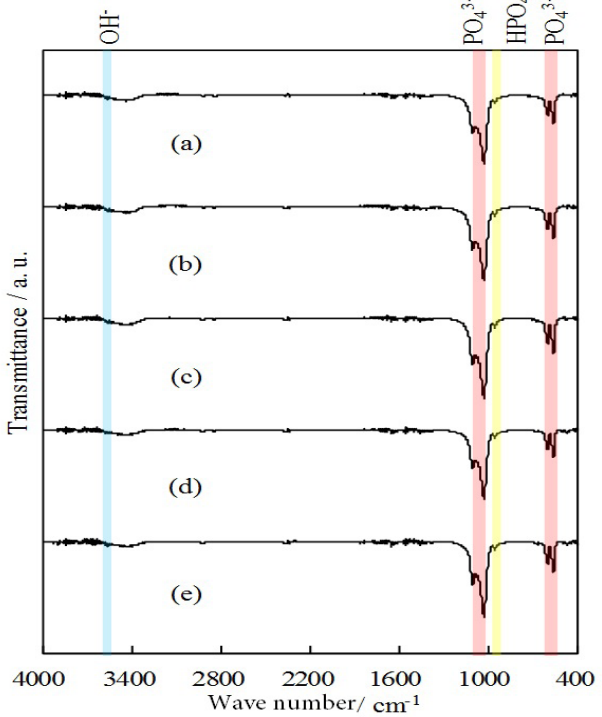

Figure 7: FT-IR spectra of the hydrothermal-treated powders for 2.5 h in a solution of 1.0 mol•dm-3 $CaCl_2$: hydrothermal temperature (a) 100, (b) 120, (c) 140, (d) 160 and (e) 180˚C.

	Synthesized powders	Hydrothermal-treated powders				
		100°C	120°C	140°C	160°C	180°C
Ca/P molar ratio	1.38	1.54	1.56	1.59	1.62	1.64

Table 3: Ca/P molar ratio of the hydrothermal-treated powders for 2.5 h in a solution of 1.0 mol•dm^{-3} $CaCl_2$.

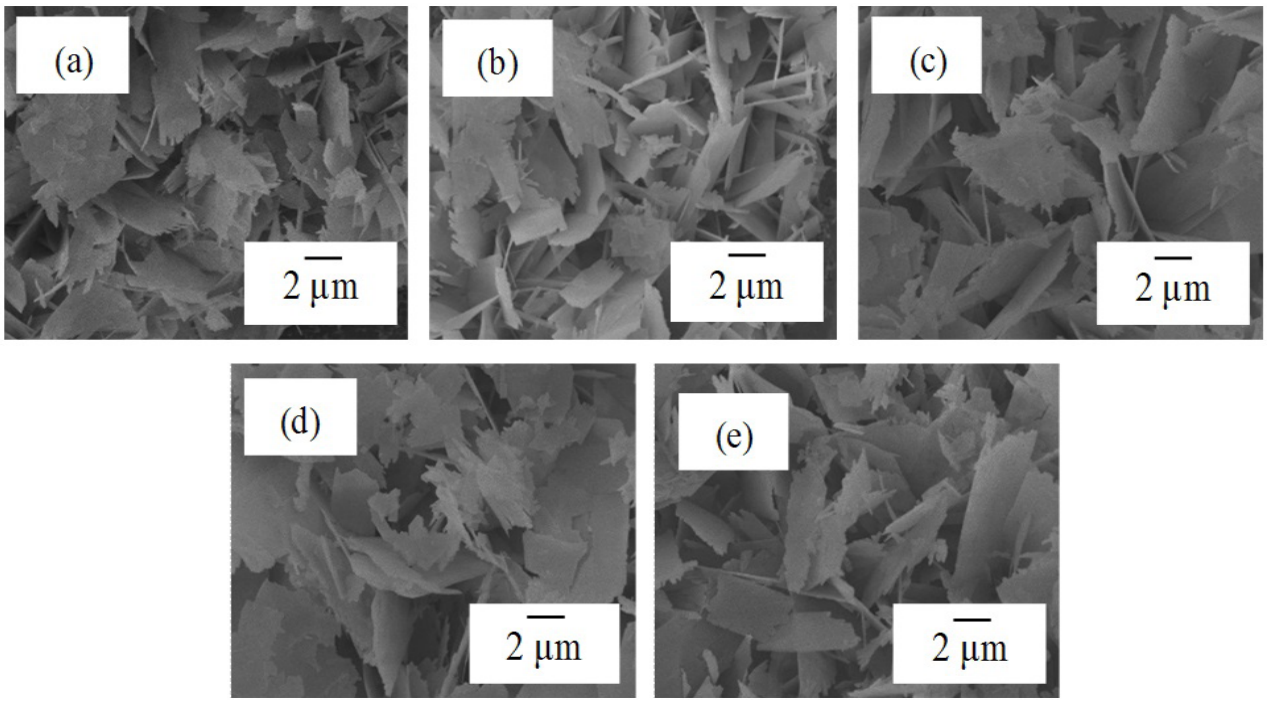

Figure 8. SEM images of the hydrothermal-treated powders for 2.5 h in a solution of 1.0 mol•dm-3 $CaCl_2$: hydrothermal temperature (a) 100, (b) 120, (c) 140, (d) 160 and (e) 180˚C.

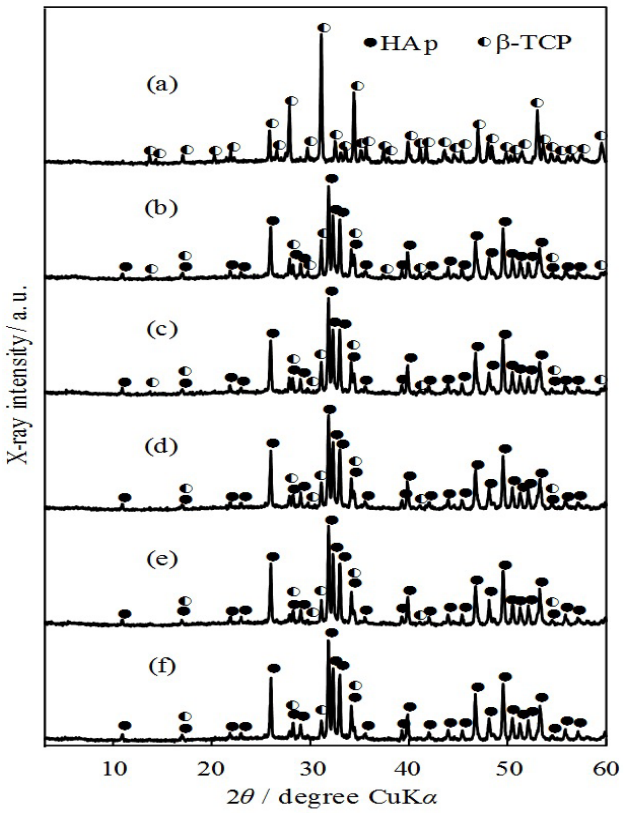

Figure 9: XRD patterns of the synthesized and hydrothermal-treated powders after heating at 1000 ˚C for 1 h: hydrothermal temperature (a) synthesized powders, (b) 100, (c) 120, (d) 140, (e) 160 and (e) 180˚C.

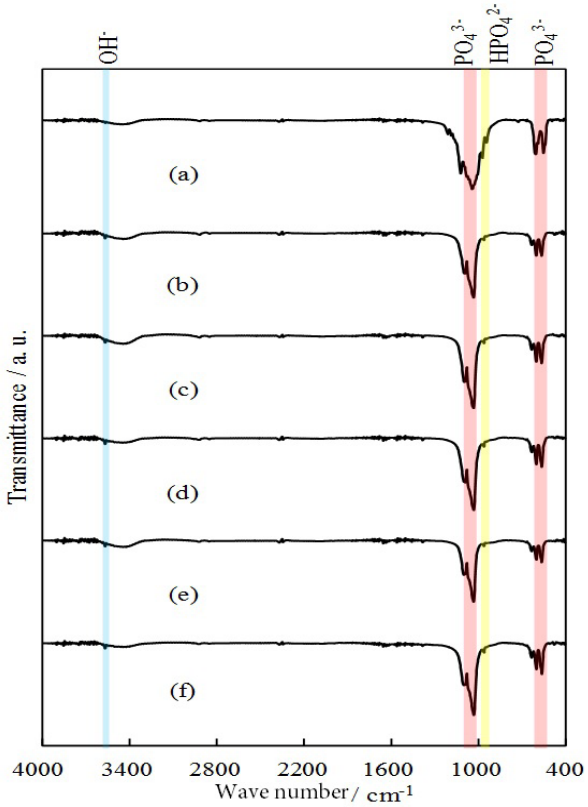

Figure 10: FT-IR spectra of the synthesized and hydrothermal-treated powders after heating at 1000˚C for 1 h: hydrothermal temperature (a) synthesized powders, (b) 100, (c) 120, (d) 140, (e) 160 and (f) 180˚C.

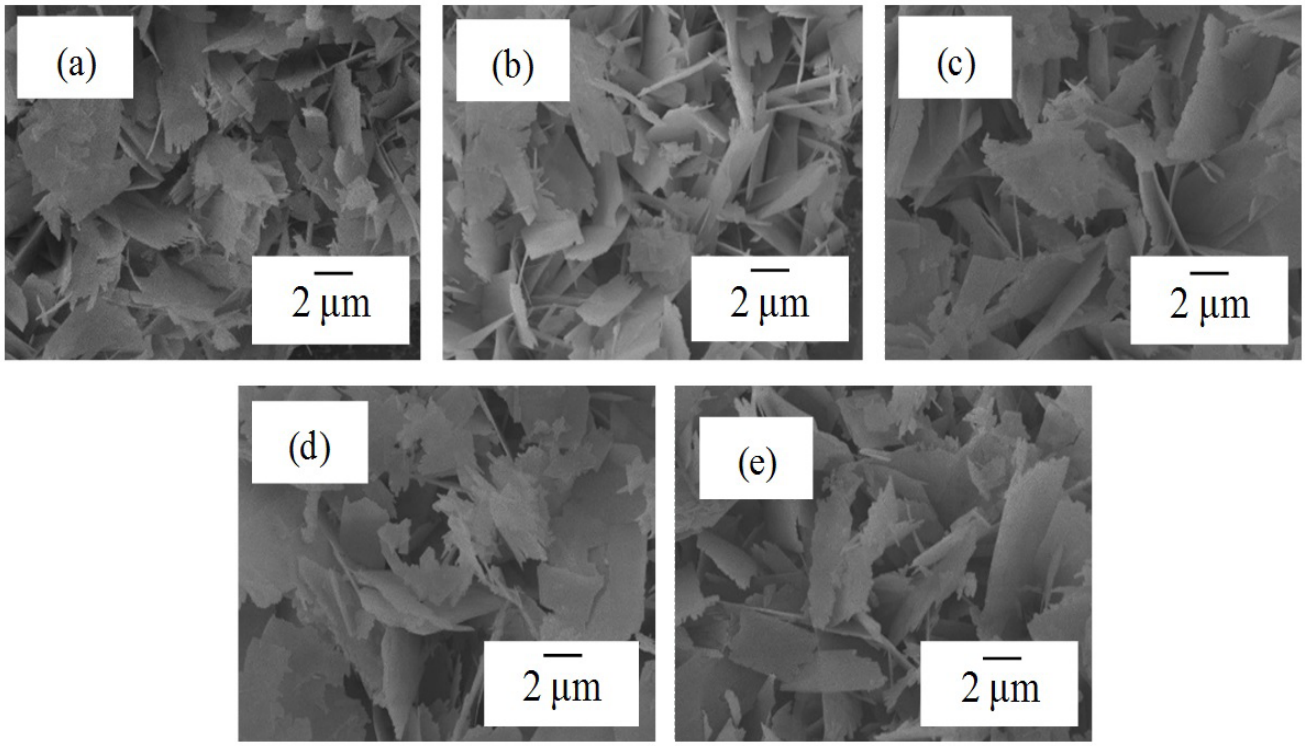

Figure 11: SEM images of the synthesized and hydrothermal-treated powders after heating at 1000 ˚C for 1 h: hydrothermal temperature (a) synthesized powders, (b) 100, (c) 120, (d) 140, (e) 160 and (f) 180˚C.

In addition to these hydrothermal conditions: the Ca^{2+} ion concentration and the hydrothermal temperature, an optimal parameter of hydrothermal time was also examined. The synthesized powders were hydrothermally treated at 180°C for 0.5, 2.5, 5, 7.5, 10 h in a solution of 1.0 mol•dm^{-3} $CaCl^2$. Results of the powder XRD patterns, the FT-IR spectra and SEM images were the same as those obtained in the section 3-2. However, the Ca/P molar ratio of the hydrothermal-treated powders was roughly constant at about 1.64 above 5 h. The hydrothermal time of 0.5 h is the best condition for simplicity of the experiment, while that of 5 h is the best condition for increasing degree of the Ca/P molar ratio. Finally, we decided that the hydrothermal time of 2.5 h was the optimal condition, which was between 0.5 h and 5 h.

Thermal stability of the synthesized and hydrothermal-treated plate-shaped HAp powders

Figure 9 shows the powder XRD patterns of the heated powders. The synthesized powders after heating were of a β-TCP single phase. Regardless of the hydrothermal temperature, the hydrothermal-treated powders after heating were of HAp and β-TCP bi-phases. The ratio of the HAp phase in the heated powders was listed in Table 4. The closer the Ca/P molar ratio of the hydrothermal-treated powders was to 1.67, the higher the ratio of the HAp phase was in those powders after heating. The FT-IR spectra of the heated powders are shown in Figure 10. In the spectrum of the synthesized powders after heating, a band at 3550 cm^{-1} assigned to hydroxide ions disappeared due to decomposition of the whole HAp crystals. Furthermore, an unknown band appeared at 950 cm-1 in the synthesized powders and at 650 cm-1 in the hydrothermal-treated powders after heating. These bands may be assigned to theP-O-P bonding in the diphosphate ($P_2O_7^{4-}$) ions [26,27]. Figure 11 shows the SEM images of the heated powders. The synthesized powders exhibited a completely broken morphology after heating. Moreover, the high Ca/P molar ratio of the hydrothermal-treated powders tended to maintain their plate-shaped morphology after heating. As listed in Table 5, there was only a marginal difference between the Ca/P molar ratio of the plate-shaped HAp powders before and after heating. From the above, increasing the Ca/P molar ratio of the plate-shaped HAp powders is effective for preventing their decomposition and morphological change after heating.

Conclusion

In order to increase the Ca/P molar ratio of the Ca-deficient plate-shaped HAp powders, the hydrothermal treatment was carried out. The Ca/P molar ratio of the plate-shaped HAp powders could be controlled in the range from 1.38 to 1.64 by the hydrothermal treatment. In particular, the Ca/P molar ratio of the plate-shaped HAp powders was raised the most using the hydrothermal conditions as follows: Ca^{2+} ion concentration of 1.0 mol•dm^{-3}, hydrothermal temperature of 180°C and hydrothermal time of 2.5 h. Moreover, making the Ca/P molar ratio of the plate-shaped HAp powders as close to 1.67 as possible greatly resulted in improving their thermal stability. From the above, the hydrothermal process may be effective for preparing the plate-shaped HAp powders with closer stoichiometric Ca/P molar ratio and developing their thermal stability.

Competing Interests

The authors declare that they have no competing interests.

Author Contributions

Yuki Mori and Mamoru Aizawa contributed to conception and design of study. Yuki Mori contributed to acquisition of data. Yuki Mori and Mamoru Aizawa contributed to interpretation of data. Yuki Mori contributed to drafting the manuscript. Mamoru Aizawa contributed to revising it.

References

1. Thian ES, Huang J, Aizawa M (2017) Nanobioceramics for Healthcare Applications. London: World Scientific Publishing Europe Ltd., The United Kingdom of Great Britain and Northern Ireland, 108 p.
2. Zhou H, Lee J (2011) Nanoscale hydroxyapatite particles for bone tissue engineering. Acta Biomater 7: 2769-2781.
3. Dorozhkin SV (2016) Calcium Orthophosphate-Based Bioceramics and Biocomposites. (1st edition), Weinheim: Wiley-VCH Verlag GmbH and Co. KGaA, Germany, 190 p.
4. Kawasaki T, Takahashi S, Ikeda K (1985) Hydroxyapatite high-performance liquid chromatography: column performance for proteins. Eur J Biochem 152: 361-371.
5. Kawasaki T, Niikura M, Kobayashi Y (1990) Fundamental study of hydroxyapatite high-performance liquid chromatography: III. Direct experimental confirmation of the existence of two types of adsorbing surface on the hydroxyapatite crystal. J Chromatogr A 515: 125-148.
6. Kawasaki T (1991) Hydroxyapatite as a liquid chromatographic packing. J Chromatogr A 544: 147-184.
7. HA Ultrogel Hydroxyapatite Chromatography Sorbent.
8. kay MI, Young RA, Posner AS (1964) Crystal structure of hydroxyapatite. Nature 204: 1050-1052.
9. Daculsi G, Kerebel B (1978) High-resolution electron microscope study of human enamel crystallites: size, shape, and growth. J Ultrastruct Res 65: 163-172.
10. Nakano T, Kaibara K, Tabata Y, Nagata N, Enomoto S, et al. (2002) Unique alignment and texture of biological apatite crystallites in typical calcified tissues analyzed by microbeam X-ray diffractometer system. Bone 31: 479-487.
11. Aizawa M, Porter AE, Best SM, Bonfield W (2005) Ultrastructural observation of single-crystal apatite fibres. Biomaterials 26: 3427-3433.
12. Aizawa M, Ueno H, Itatani K, Okada I (2006) Syntheses of calcium-deficient apatite fibres by a homogeneous precipitation method and their characterizations. J Eur Ceram Soc 26: 501-507.

	Synthesized powders	Hydrothermal-treated powders				
		100°C	120°C	140°C	160°C	180°C
Ratio of the HAp phase / %	0	79	82	85	88	90

Table 4: Ratio of the HAp phase in the synthesized and hydrothermal-treated powders after heating at 1000°C for 1 h.

	Synthesized powders	Hydrothermal-treated powders				
		100°C	120°C	140°C	160°C	180°C
Ca/P molar ratio	1.39	1.55	1.57	1.60	1.62	1.64

Table 5: Ca/P molar ratio of the synthesized and hydrothermal-treated powders after heating at 1000°C for 1 h.

13. Yoshimura M, Suda H, Okamoto K, Ioku K (1994) Hydrothermal synthesis of biocompatible whiskers. J Mater Sci 29: 3399-3402.

14. Zhu R, Yu R, Yao J, Wang D, Ke J (2008) Morphology control of hydroxyapatite through hydrothermal process. J Alloy Compd 457: 555-559.

15. Zhang H, Darvell BW (2010) Synthesis and characterization of hydroxyapatite whiskers by hydrothermal homogeneous precipitation using acetamide. Acta Biomater 6: 3216-3222.

16. Zhang H, Darvell BW (2011) Morphology and structural characteristics of hydroxyapatite whiskers: effect of the initial Ca concentration, Ca/P ratio and pH. Acta Biomater 7: 2960-2968.

17. Ban S, Maruno S (1998) Morphology and microstructure of electrochemically deposited calcium phosphates in a modified simulated body fluid. Biomaterials 19: 1245-1253.

18. Ban S, Hasegawa J (2002) Morphological regulation and crystal growth of hydrothermal-electrochemically deposited apatite. Biomaterials 23: 2965-2972.

19. Zhuang Z, Yamamoto H, Aizawa M (2012) Synthesis of plate-shaped hydroxyapatite via an enzyme reaction of urea with urease and its characterization. Powder Technol 222: 193-200.

20. Sathish M, Miyazawa K (2007) Size-tunable hexagonal fullerene (C60) nanosheets at the liquid-liquid interface. J Am Chem Soc 129: 13816-13817.

21. Bai X, Zheng L, Li N, Dong B, Liu H (2008) Synthesis and characterization of microscale gold nanoplates using langmuir monolayers of long-chain ionic liquid. Cryst Growth Des 8: 3840-3846.

22. Wang CW, Ding HP, Xin GQ, Chen X, Lee YI, et al. (2009) Silver nanoplates formed at the air/water and solid/water interfaces. Colloids Surf A 340: 93-98.

23. Chen KC, Wang CW, Lee YI, Liu HG (2011) Nanoplates and nanostars of ß-PbO formed at the air/water interface. Colloids Surf A 373: 124-129.

24. Zhuang Z, Yoshimura H, Aizawa M (2013) Synthesis and ultrastructure of plate-like apatite single crystals as a model for tooth enamel. Mater Sci Eng C Mater Biol Appl 33: 2534-2540.

25. Byrappa K, Yoshimura H (2013) Handbook of Hydrothermal Technology. (2nd edition), New York: William Andrew, Inc., The United States of America, 37 p.

26. Grayson M, Griffith EJ (1969) Topics in Phosphorus Chemistry. New Jersey: John Wiley and Sons, The United States of America, 282 p.

27. Raynaud S, Champion E, Bernache-Assollant D, Thomas P (2002) Calcium phosphate apatites with variable Ca/P atomic ratio I. Synthesis, characterisation and thermal stability of powders. Biomaterials 23: 1065-1072.